Bull. Soc. géol. France, 2013, t. 184, n° 4-5, pp. 335-346

Rupture propagation in strong earthquake sources and tectonic stress field

YU.L. REBETSKY and R.E. TATEVOSSIAN

Keywords. – Stresses, Rock failure, Rupture propagation, Strong earthquakes

Abstract. – Problems of physical basis of earthquake source mechanics are discussed. Results of stress state reconstruction based on the cataclastic analysis of discontinuous dislocations in some seismotectonic active earth crust domains are presented. Common features of the stress state in areas of preparation of strong earthquake in this century are revealed. It is demonstrated that the distribution of the effective isotropic pressure and of the maximal shear stress in areas of earthquake source preparation is characterized by essential heterogeneity. The main part of the source is always associated to crust domain under low effective confining pressure. Specific role of crust domains characterized by high stress gradients is recognized. The nucleation point of the earthquake is usually associated to such domains. Based on some strong earthquake case studies it is demonstrated that usually the *rupture propagates* from the region of high gradients of stresses toward the crust domains characterized by low effective compression.

Propagation de la rupture dans les sources de fort tremblement de terre et le champ de contraintes tectoniques

Mots-clés. – Contraintes, Rupture des roches, Propagation de la rupture, Forts séismes

Résumé. – Dans cet article, nous discutons de problèmes qui concernent les fondements physiques de la mécanique de la source sismique. Les résultats de la reconstruction de l'état de contrainte fondée sur la méthode d'analyse cataclastique des dislocations discontinues dans certaines régions sismo-tectoniquement actives de la croûte terrestre sont présentés. Des caractéristiques communes aux régions de préparation d'un fort séisme durant ce siècle sont illustrées. Nous montrons que la distribution de la pression isotrope effective et de la contrainte cisaillante maximale dans les secteurs de préparation d'un séisme se caractérise par une hétérogénéité importante. La majeure partie de la source correspond toujours à un domaine crustal soumis à une pression de confinement effective faible. Nous caractérisons également le rôle spécifique des domaines crustaux associés à de forts gradients de contraintes. Le point de nucléation du séisme est généralement associé à de tels domaines. En étudiant quelques exemples de forts séismes, nous montrons que la rupture se propage généralement depuis la région de forts gradients de contraintes vers les portions de croûte caractérisées par une compression effective faible.

INTRODUCTION

We should agree that we still do not have clear understanding of conditions defining possibility of starting the process of brittle failure at large scale – the earthquake. From laboratory experiments we know the conditions when the micro crack is nucleated, but we do not know the conditions which define its ability to grow up to tens and hundred kilometers and to become a shear fault. Default assumption is that strength criteria defining occurrence of the crack at micro- and macroscales (fracture of millimeters up to centimeters) and at mega scale (tens of kilometers) are the same, i.e. brittle failure has fractal properties. From this assumption follows that all the volume of strong earthquake source preparation having tens of kilometers is characterized by high level of deviatoric stresses [Reid, 1910; Scholz *et al.*, 1973; Mjachkin *et al.*, 1975; Sadovsky and Pisarenko, 1985; Kasahara, 1981; Kossobokov and Keilis-Borok, 1990; Sobolev, 1993]. It is supposed that the stresses and deviatoric elastic deformation grow because of asperities. The earthquake results in the breaking of the asperity and in the drop of accumulated energy of elastic deformation.

From the other hand, experimental data on rocks [Mogi, 1966; Byerlee, 1968; Brace, 1978; Stavrogin and Protosenia, 1992] have demonstrated that brittle strength depends on the level of confining pressure and that the high level of deviatoric stresses which can stand the rock specimen corresponds also to high confining pressure. We also know that when confining pressure grows, the elastic deformation drop (shear stress-drop) decreases, and consequently, the energetic efficiency of the brittle failure decreases. At a certain level of confining pressure brittle failure is impossible at macroscopic level and energy dissipation of deviatoric elastic deformation is transferred to the level of grains and crystals, which corresponds to plasticity.

If extrapolating these results of laboratory experiments at large scales, we can state that crust domains characterized by high stresses (confining pressure and deviatoric stresses) should be interpreted as volumes where the development of a large earthquake is difficult. Here aseismic creeping along faults, many weak earthquakes and other small-scale dissipative phenomena related to other stress-state scale can occur.

1. IPE RAS, 123995 GSP-5, B. Gruzinskaya, 10/1, Moscow, Russia
Manuscript received on March 15, 2012; accepted on October 27, 2012

Because of this peculiar feature of the stress state defining the possibility of brittle failure, Rice [Rice, 1969] proposed that the domains where a strong earthquake is prepared are characterized by intermediate level of stresses to which correspond areas of intermediate level of friction on faults. A high stress drop corresponds to such a stress state on experimental failure diagrams.

Another questionable point is the extrapolation of critical stress-state criteria obtained from macroscopic level to megascopic level. The problem is that continuum mechanics cannot describe phenomena at micro-level, where the concept of continuum itself is conventional. Macroscopic strength criteria are based on the quasi-homogeneity of the stress state at macroscopic crack scale. In the reality strain state at micro scale is essentially heterogeneous [Panin, 1998]. We use standard macroscopic strength criteria because we do not have anything else.

Studying the heterogeneities of stress distribution at microscopic scale preceding development of the macroscopic crack is very difficult because of media heterogeneity, and it requires special devices and special mathematical tools. The stress state at large scale of seismic faults can help us to solve the problem. How are stresses before the strong earthquake occurrence distributed?

Methods of tectonophysic analysis of discontinuous dislocations applied to the evaluation of stress parameters in nature which are developing since mid of the last century can be helpful. There are a set of methods using seismological data on earthquake mechanisms and geological data on fault striations [Arthaud, 1969; Pegararo, 1972; Angelier, 1975, Goustchenko, 1975; Carey, 1976; Reches, 1978; Lisle, 1979; Yunga, 1979; Etchecopar *et al.*, 1981; Michael, 1984; Gephard and Forsyth, 1984; Gintov and Isai, 1984; Rivera and Cirsternas, 1990; Jamaji, 2000; among others]. But among these methods studying stresses in natural conditions only few are evaluating stress values [Reches, 1987; Angelier, 1989; Hardebeck and Hauksson, 2001; Gintov, 2005; Rebetsky, 2007a].

METHOD OF CATACLASTIC ANALYSIS OF DISCONTINUOUS DISLOCATIONS

In the IPE RAS the method of cataclastic analysis (MCA) of set of discontinuous dislocations has been developed [Rebetsky, 2007a]. It defines all components of the stress tensor averaged at the scale, which corresponds to the seismological data on earthquake mechanisms. The MCA incorporates several stages of evaluation of stress parameters. Only some part of tensor components is defined at each stage. Data on earthquake source mechanisms are used in a first stage; generalization of results of rock sample failure in laboratory experiments in a second stage; seismological data on stress drop in earthquake sources in a third stage; impulse conservation law in vertical direction in a fourth and last stage.

First stage of the MCA

The orientation of principal stress axes [Rebetsky, 1996, 1997, 1999, 2001] and the parameter Φ defining the ratio of the deviatoric components of the stress tensor are evaluated. Energy conditions of theory of plasticity which require dissipation of internal strain energy at each shear crack (Eq. (1) and (2)) are the basis of this stage of the MCA. They recognize as the true stress tensor the one which ensures maximum dissipation of this energy during the process of plastic flow. To define it, the stress tensor components and increments of seismotectonic deformations are calculated as being mutually consistent.

One of the important routines of the MCA is the recognition of earth crust domains characterized by a quasi-homogeneous stress state. There are criteria (Eq. 3) which can be used to distinguish if earthquake source mechanisms located close to one another can be addressed as "homogeneous sample set". Also these criteria are consequences of energy conditions of plasticity theory; they superimpose stronger constraints on earthquake source mechanism sample set homogeneity than the type of criteria used in [Angelier and Mechler, 1977].

Thus, after the first stage, the orientation of principal stress axes and the increment of seismotectonic deformations together with the ratio of deviatoric components of principal corresponding tensors are defined in each quasi-homogeneous domain. Note, that after the first stage, sample set of earthquake source mechanisms characterizing quasi-homogeneous phase of deformation is defined. These homogeneous sample sets are used at the second stage of the stress reconstruction.

At this stage the MCA algorithm is close to the methods by Pegararo [1972], Carey [1976], Angelier and Mechler [1977], and which is known as the right dihedra method. In the MCA method, as in the method of right dihedra, each shear crack superimposes constraints on the orientation of principal axes of maximal compression σ_3 and minimal compression (deviatoric tension) σ_1. In the MCA, inequalities, which define possible orientation of principal stress axes are derived from fundamental standpoint of the plasticity theory on coherency of stress tensor components and increment of plastic deformations [Chernykh, 1988]:

$$(\sigma_i - \sigma_j)(de_{ii}^p - de_{jj}^p) \geq 0,\ i,\ j\ =\ 1,\ 2,\ 3 \qquad (1)$$

where de_{ii}^p are the components of plastic strain elongation and shortening increment in the direction of principal stress axes σ_i. From (1) and according to the condition $\sigma_1 \geq \sigma_2 \geq \sigma_3$ (tensions positive) assumed in geodynamics it clearly follows that:

$$de_{11}^p \geq de_{22}^p \geq de_{33}^p,\ \text{where}\ de_{11}^p + de_{22}^p + de_{33}^p = 0 \qquad (2)$$

According to (2), irreversible plastic elongation and shortening strains in the direction of principal stress axes are defined according to the indexes of axes. 1) In the direction of σ_1 elongation occurs. 2) In the direction of σ_3 shortening occurs. 3) In the direction of σ_2 either elongation or shortening can occur but their modulus has to be smaller than strains along other principal axes.

In the MCA it is assumed that conditions (2) are valid for each episode of irreversible strain that occurred through dislocations along individual cracks and faults (hypothesis I). Using expressions for increments of irreversible deformations caused by shear crack [Kostrov and Das, 1988] after referring them to the coordinate system linked to principal axes of searched stress tensor σ_i (i = 1, 2, 3), inequalities (2) can be rewritten as:

$$\ell_{n1}^{\alpha}\ell_{s1}^{\alpha} \geq \ell_{n2}^{\alpha}\ell_{n2}^{\alpha} \geq \ell_{n3}^{\alpha}\ell_{n3}^{\alpha}\ \text{where}$$
$$\ell_{n1}^{\alpha}\ell_{s1}^{\alpha} + \ell_{n2}^{\alpha}\ell_{n2}^{\alpha} + \ell_{n3}^{\alpha}\ell_{n3}^{\alpha} = 0 \qquad (3)$$

ℓ^{α}_{ni} and ℓ^{α}_{si} (i = 1, 2, 3) are the directing cosines of the unit vector normal to the crack plane ***n*** and the dislocation vector ***s*** to three principal stress axes.

In the MCA, inequalities (3) are assumed to be criteria for compiling homogeneous sets of earthquake mechanisms, which are used to define parameters of stress tensor for quasi-homogeneous domains. In the same manner as it is done in the right dihedra method, but using expression (3) and data on earthquake mechanisms it is possible to locate on the unit hemisphere areas where the principal stress axes of the searched stress tensor can be. In the MCA, for the calculation of coefficient Φ we use the requirement that energy of elastic deformation dissipation has to reach its maximum through discontinuous dislocations [Rebetsky, 1997].

Therefore, at the first stage of the MCA three Euler's angles and coefficient Φ defining the location of the principal stress axes and stress ellipsoid are defined. Additionally, for each crust domain for which these parameters of stress tensor are defined a corresponding set of earthquake mechanisms is compiled. Based on this set the other components of the stress tensor will be determined.

SECOND STAGE OF THE MCA

The main idea of the second stage is based on well-known results obtained in the experiments of rock failure under three-axial loading in laboratory conditions. Higher the level of confining pressure, higher has to be the level of stresses to achieve the failure, i.e. the level of confining pressure and level of maximal shear stresses are correlated and are consistent with rock strength parameters.

Higher the confining pressure, lower will be the variations in orientations of cleavage planes in samples with preliminary introduced defects having different orientations. When the confining pressure is low, practically all strength defects oriented in different directions are activated even under relatively low axial pressure (the whole area of grey color within the Mohr's big circle and out of small circles in fig. 1a). In this case the scatter in orientation of cleavage planes is maximal. Under very high confining pressure, the location of the cleavage planes practically coincides with the plane corresponding to the angle of internal friction in rocks (in the vicinity of the point A in fig. 1a). Therefore, fault direction scatter carries information on the level of confining pressure and deviatoric stresses. Analysis of scatter of points characterizing stresses on cleavage planes on Mohr's diagram was made also in [Angelier, 1989].

According to Terzaghi [1943] for samples containing fluids (condensate at depths) in cracks and pores one can discuss the relationship between effective pressure and deviatoric stresses. Under effective pressure the difference between tectonic pressure in rock solid frame and fluid pressure in crack and pore space, is considered.

The line of minimal friction (point K in fig. 1b) and relative values of effective pressure and maximal shear stresses (see Eq. 10) is defined on Mohr's diagram for the earthquakes from homogeneous sample set. Here, the parameters are normalized on the unknown value of rock massive internal cohesion strength, which has to be smaller than the values obtained in laboratory experiments on rock failure.

Normal and shear stresses acting over nodal planes $\mathbf{n}^{\alpha}$ and $\mathbf{s}^{\alpha}$ (α - is sequential number of event in the set) of earthquake source mechanisms for each homogeneous set are analyzed [Rebetsky, 2003, 2005a, b]. It is assumed that the real acting plane from two nodal planes of earthquake source mechanism is the one for which the Coulomb's stress C has the maximal value (hypothesis 2):

$$MAX\left[C^{\alpha}_{n};C^{\alpha}_{s}\right] \text{ for } C^{\alpha}_{n}=\tau^{\alpha}_{n}-k_{s}\sigma^{*\alpha}_{nn},$$
$$C^{\alpha}_{s}=\tau^{\alpha}_{s}-k_{s}\sigma^{*\alpha}_{ss},\ \sigma^{*\alpha}_{ii}<0,\ \tau^{\alpha}_{i}>0,\ i=n,\ s \qquad (4)$$

Here τ^{α}_{n} and $\sigma^{*\alpha}_{nn}$ are the shear and normal stresses acting over nodal plane having normal; $\mathbf{n}^{\alpha}$; τ^{α}_{s} and $\sigma^{*\alpha}_{ss}$ the same over nodal plane having normal $\mathbf{s}^{\alpha}$. σ^{*}_{ii} is the effective normal stress, in which the contribution of the fluid pressure in cracks p_{fl} is taken into account ($\sigma^{*\alpha}_{nn}=\sigma^{\alpha}_{nn}+p_{fl}$) [Terzaghi, 1943].

At this stage, the zone of brittle failure on Mohr's diagram (fig. 1a and fig. 13 from Mogi[1966] is used to evaluate the relative values of stresses. This zone is between two characteristic lines defining limits of internal strength and minimal static friction:

$$\tau_{n}-k_{f}\sigma^{*}_{nn}=T_{f},\ \tau_{n}-k_{s}\sigma^{*}_{nn}=0 \qquad (5)$$

where T_f is the strength of the internal cohesion; k_f and k_s are the coefficients of the internal and the static friction (in the MCA it is assumed that $k_f = k_s \approx 0.5 - 0.6$). Algorithm of MCA assumes that T_f and k_f are constant.

The points characterizing stresses over pre-existing and reactivated faults α from homogeneous set lie within the zone of brittle failure (area between two lines on fig. 1a):

$$\tau^{\alpha}_{n}+k_{s}\sigma^{*\alpha}_{nn}=T^{\alpha}_{n} \text{ for } 0\le T^{\alpha}_{n}\le T_{f} \quad \tau^{\alpha}_{n}\ge 0,\ \sigma^{*\alpha}_{nn}\le 0 \qquad (6)$$

where T^{α}_{n} is the strength of surface adhesion for the crack number α.

Using the first expression in (5) together with the relationship between stresses acting over the faulting plane and principal stresses [Jager, 1962], one can find the relationship between the maximal shear stress τ ($\tau=(\sigma_1-\sigma_3)/2$) and the effective pressure p^* ($p^*=p-p_{fl}$, $p=-(\sigma_1+\sigma_2+\sigma_3)/3$:

$$\tau=\frac{\left(T_f+k_f p^*\right)}{\operatorname{cosec} 2\varphi_f-k_f\mu_\sigma/3} \text{ for } ctg2\varphi_f=k_f,\ \mu_\sigma=2\Phi-1 \qquad (7)$$

From (7) it comes that we need one more equation for evaluating τ and p^*. To compile it, in the MCA it is assumed (hypothesis 3) that in the homogeneous set of earthquakes there is always an event for which Coulomb's stresses are equal to the minimal resistance of friction (second expression in (5)). Under this hypothesis and using the expression for stresses through their reduced values, one can write:

$$\sigma^{*\alpha}_{nn}=\sigma^{*}_{o}+\tau\tilde{\sigma}^{\alpha}_{nn};\ \tilde{\sigma}^{\alpha}_{ns}=\tau\tilde{\sigma}^{\alpha}_{ns} \text{ for } \sigma^{*}_{o}=-\left(p^{*}+\frac{\mu_\sigma}{3}\tau\right) \qquad (8)$$

where $\tilde{\sigma}^{\alpha}_{ng}=(1-\mu_\sigma)\ell^{\alpha}_{1n}\ell^{\alpha}_{1g}-(1-\mu_\sigma)\ell^{\alpha}_{3n}\ell^{\alpha}_{3g}+\delta_{ng}\mu_\sigma$, $g=n,s$

Then one gets:

$$\frac{p^*}{\tau}=\frac{1}{k_s}\left(\tilde{\sigma}^{K}_{nt}+k_s\tilde{\sigma}^{K}_{nn}\right)-\frac{\mu_\sigma}{3} \qquad (9)$$

The index K in the reduced stresses $\tilde{\sigma}^{K}_{nt}$ and $\tilde{\sigma}^{K}_{nn}$ corresponds to the event number in homogeneous set which is located on the line of minimal friction on the Mohr's diagram (fig. 1b).

Using (7) and (8) we get:

$$\left\langle \frac{\tau}{T_f} \right\rangle = \frac{1}{\sec 2\varphi_s - \left(\tilde{\sigma}_{nt}^K + k_s \tilde{\sigma}_{nn}^K\right)};$$
$$\left\langle \frac{p^*}{T_f} \right\rangle = \frac{\tilde{\sigma}_{nt}^K + k_s \tilde{\sigma}_{nn}^K - k_s \mu_\sigma / 3}{k_s \left[\sec 2\varphi_s - \left(\tilde{\sigma}_{nt}^K + k_s \tilde{\sigma}_{nn}^K\right)\right]} \qquad (10)$$

Triangle brackets in (10) indicate that the ratio is defined but not the individual values of τ, p^* and T_f.

Thus, after the second stage of the MCA, the stress tensor components can be written in the following form:

$$\sigma_{nn}^{*\alpha} = \left[\left\langle \frac{\sigma_o^*}{T_f} \right\rangle + \left\langle \frac{\tau}{T_f} \right\rangle \tilde{\sigma}_{nn}^\alpha\right] T_f;\ \sigma_{nt}^\alpha = \left\langle \frac{\tau}{T_f} \right\rangle \tilde{\sigma}_{nt}^\alpha T_f$$
$$\sigma_o^* = \left[\left\langle \frac{p^*}{T_f} \right\rangle + \frac{\mu_\sigma}{3}\left\langle \frac{\tau}{T_f} \right\rangle\right] T_f \qquad (11)$$

where expressions in triangle brackets are according to (10) (second stage of the MCA) and reduced stresses $\tilde{\sigma}_{nt}^\alpha$ and $\tilde{\sigma}_{nn}^\alpha$ defined at the first stage.

We should note that a similar analysis for evaluation of stresses on Mohr's diagram based on striation data from geological faults was conducted in Reches [1987] and Angelier [1989].

Third stage of the MCA

The problem to be solved at the MCA third stage is the definition of the unknown cohesion strength of rock massifs. We assume that cohesion strength is constant in the region being averaged within the volumes not smaller than the volumes used to average stresses in reconstruction procedure at the MCA first two stages. After the second stage, the stress drop in strong earthquake sources can be defined up to normalization to yet unknown cohesion strength. This, together with the above formulated assumption on constancy of cohesion strength in rocks within various areas of the study region, makes it possible to calculate the cohesion strength if data on stress drop for one or two strong earthquakes in the region are available. Seismologists can get such data from the analysis of source spectra [Castro *et al.*, 1990] for relatively large earthquakes (M > 6). In Hardebeck and Hauksson[2001] data on stress drop were used to evaluate tectonic stress level in the source zone of the Landers earthquake.

Thus, after the third stage, deviatoric components of the stress tensor and effective pressure are defined. Still unknown are tectonic and fluid pressures, the difference of which defines the effective stress.

It comesfrom (11) that after the first two stages the parameters of the effective stress tensor are determined as normalized to the unknown strength T_f. Data on stress drop in largest earthquake sources of the region are used to determine T_f. at the third stage of the MCA [Rebetsky and Marinin, 2006a,b; Rebetsky, 2007a].

Shear stresses acting on the fault plane before its activation $\tau_n^{\alpha 0}$ and after slip along it $\tau_n^{\alpha 1}$ can be written in the following form:

$$\tau_n^{\alpha 0} = T_s^\alpha - k_f \left\langle \frac{\sigma_{nn}^{*\alpha 0}}{T_f} \right\rangle T_f,\ \tau_n^{\alpha 1} = -k_k \left\langle \frac{\sigma_{nn}^{*\alpha 1}}{T_f} \right\rangle T_f \qquad (12)$$

k_k is the coefficient of kinematic sliding friction acting on crack when its sides move (in the MCA $k_f - k_k = 0.1$).

According to the results of theoretical studies of stresses generated by the fault in elastic body [Osokina, 1988], stresses normal to a fault plane do not alter before and after its activation $\sigma_{nn}^{\alpha 0} = \sigma_{nn}^{\alpha 1}$ (fig. 1a) Extrapolating this result to the effective normal stresses (hypothesis 4) one gets expression for the stress drop on the fault plane from (12) (α is event number from homogeneous set:

$$\Delta\tau_n^\alpha = T_f - \left(k_f - k_k\right)\left(\tilde{\sigma}_{nn}^\alpha \left\langle \frac{\tau}{T_f} \right\rangle - \left\langle \frac{\sigma_o^*}{T_f} \right\rangle\right) T_f \qquad (13)$$

Thus, for each earthquake it is possible to assess the stress drop up to the known value of internal cohesion T_f of rock massive. If the stress drop for an earthquake is known (usually, these are the strongest earthquakes in the region) based on seismological data, by substitution in the right hand of (13) it is possible to evaluate T_f.

We should note that the expression (13) is for the case when direction of slip of the crack sides coincides with the direction of shear stresses on it before activation. It is not always the case. But it is not difficult to get the expression for the more general case.

Note that the possible use of data on stress drop for evaluating the levels of stresses in the source zone of the 1994 Landers earthquake (California, USA) has already been suggested by [Hardebeck and Hauksson, 2001].

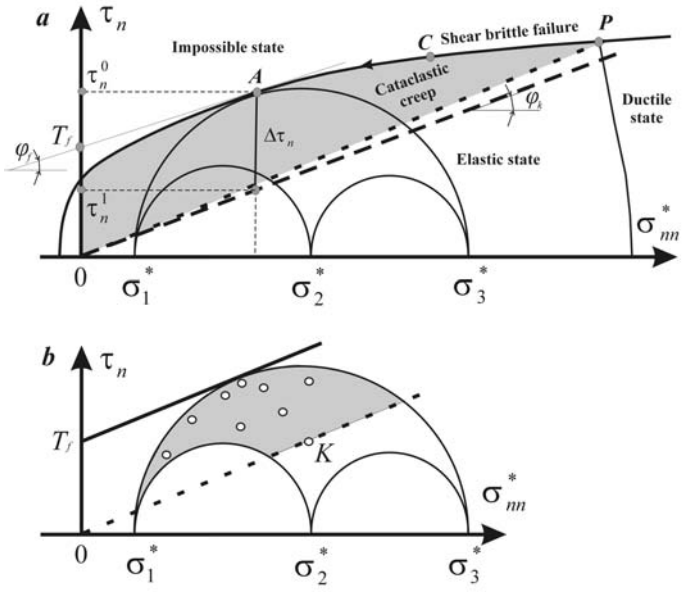

FIG. 1. – Generalized experimental (a) and simplified (b) Mohr's diagrams (negative values of stresses are shown in right direction).
a – Mohr's diagram and evaluation of stresses released in the earthquake source: *P* is the point indicating the end of the brittle failure area located between the external envelope (solid line) and line of minimal static friction (dashed line). *A* is the point of maximal stress-drop (vertical line between the envelope and dashed-and-dotted line – resistance of forces of kinematic friction). τ_n^0 and τ_n^1 are shear stresses on the fault plane before and after fault activation. The arrows from point C on the external envelope show the direction of preferred failure propagation, when it occurs in areas of higher stresses. Light grey is the area of brittle failure for any stress state.
b – Simplified Mohr's diagram in the framework of MCA: the solid line is the external envelope, the dashed line corresponds to the minimal static friction. White circles are the points of stresses on the fault plane from homogeneous sample. K is the point with minimal strength. Light grey is the area of brittle failure for a given stress state.

Fourth stage of the MCA

Equation of conservation of impulse in vertical direction (Eq. 15) written with the approximation of thick plates is used to determine the tectonic pressure. This equation is written for each quasi-homogeneous domain; it links in differential form all previously calculated stress tensor components and unknown value of tectonic pressure. The results of this stage are data on tectonic pressure and fluid pressure for each quasi-homogeneous domain within the averaged corresponding to averaging of deviatoric stress components. In Sibson [1974] it was suggested to use equation of the impulse conservation in vertical direction for determination of stress values. The equation was simplified to the hypothesis of that stresses acting on horizontal planes are equal to upper layer rock weight.

Dividing effective pressure (p^*) on fluid pressure (p_{fl}) and on tectonic pressure (p) is carried at this stage [Rebetsky, 2009a, b, c]. Equalities of conservation of impulse in vertical direction formulated in the approximation of thick plates are used [Love, 1927]. The algorithm takes into account the impact of lateral gradient of shear stresses σ_{sz} on the vertical stresses σ_{zz} acting on horizontal planes:

$$p = \gamma_c (0.5H_c + h_c) + \tau\overline{\sigma}_{zz} + 0.5H_c \frac{\partial}{\partial s}(\overline{\sigma}_{sz}\tau)$$
$$\text{and } p_{fl} = p - p^* \qquad (15)$$

where $\overline{\sigma}_{zz}$ is the reduced vertical stress ($\sigma_{zz} = -p + \tau\overline{\sigma}_{zz}$), γ_c is the mean density of crustal rock, H_c is the mean crustal thickness, h_c is the crustal topography and s is the direction of shear stress on the horizontal plane ($\sigma_{sz} = \pm\sqrt{\sigma_{xz}^2 + \sigma_{yz}^2}$).

This factor (15) was not considered in the hypothesis that the vertical stress equals the weight of the overlying rocks assumed by Sibson [1974] in his algorithm for the evaluation of stresses.

Thus, by incorporating results of experiments on rock failure and additional seismological data into the analysis, the MCA makes it possible to evaluate not only the components of stress tensor but also the strength of the rock massifs. Such a tool for evaluating stresses and rock strength in the natural conditions essentially enlarges perspectives of studying regularities in earthquake source preparation and development of earthquake source physics.

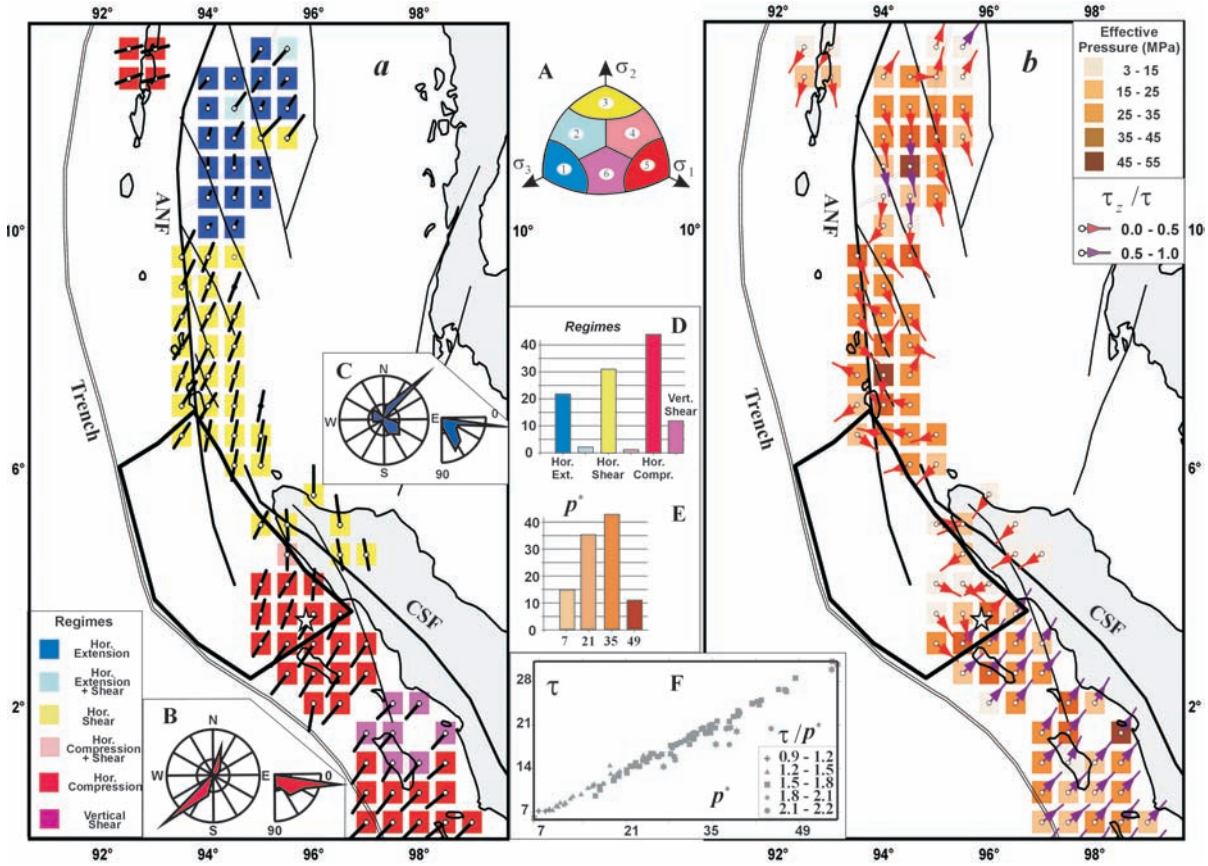

FIG. 2. – Stress state parameters in the earth crust in the western flank of Sunda island.
a – geodynamic type and projection of dip of maximal compression axis σ_3 (length of the vector is shorter for steeper dip; circle is the starting point; the circle is in the middle for sub-horizontal position of axis – ±15°);
b – effective pressure and orientation of axis and relative values of underthrusting shear stresses τ_z (normalized to the maximum shear stress τ).
Star is the nucleation point of the main shock; polygon contours first 420 km in of the rupture. Faults are shown according to [Hain and Lomize, 1995]: CSF – Central Sumatra fault, PA – pull-apart structures of the back-arc basin, ANF – Andaman-Nicobar fault.
In the insets are shown: A – the scheme of identification of the geodynamic regime using the octant built on the principal stress axis according to the orientation of axis toward zenith (1 – horizontal compression, 3 – horizontal shear, 5 – horizontal extension, 2 – horizontal compression and shearing, 4 – horizontal extension and shearing, 6 – shearing in vertical plane); B and C , circular diagrams of occurrences of different values of strike azimuths and dip angles of principal stress axes σ_3 and σ_1 correspondingly; D – diagram of occurrences of geodynamic regime types in domains; E – diagram of occurrences of effective pressure p^* in domains; F – plot of modulus of maximal shear stresses versus effective pressure.

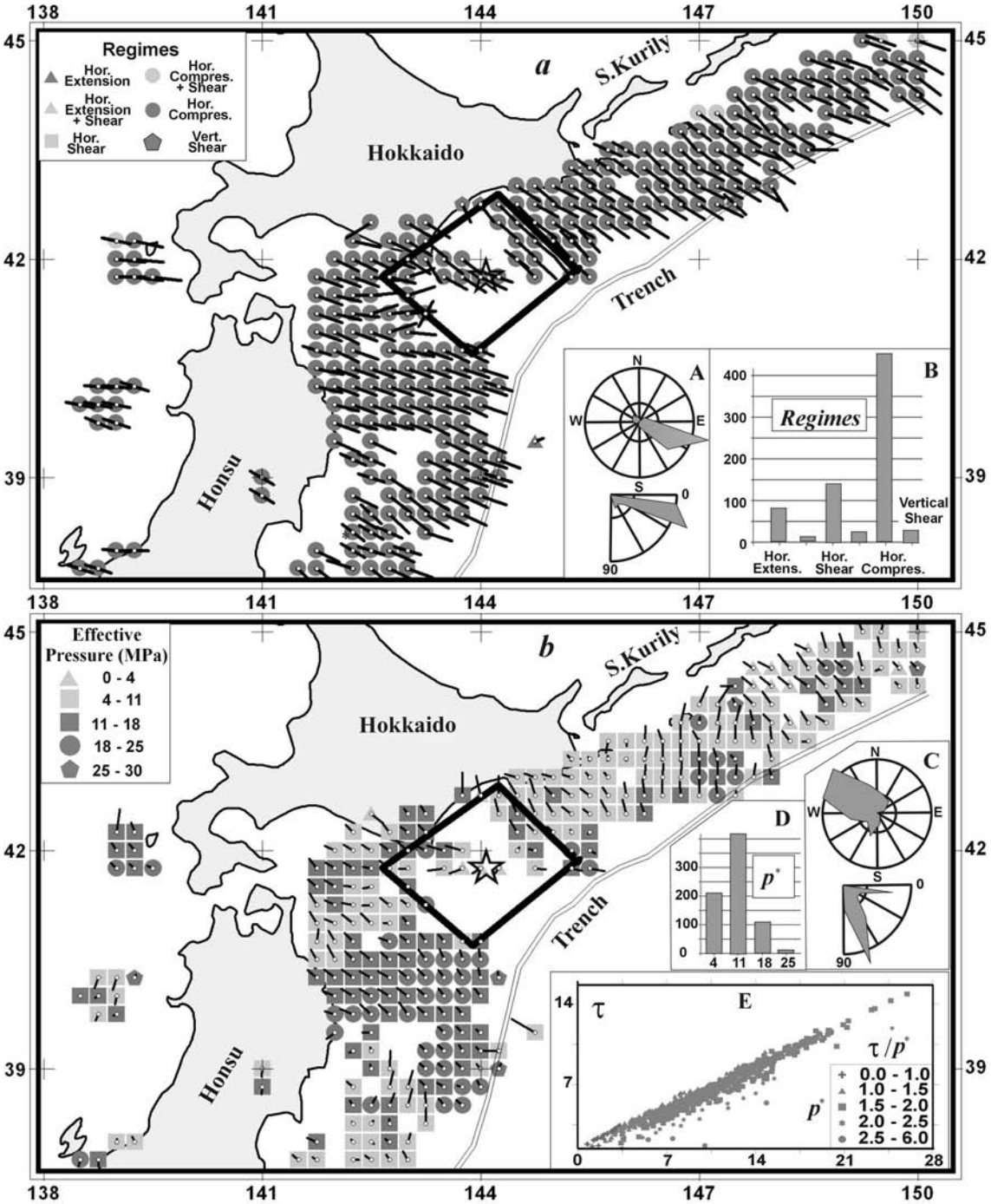

FIG. 3. – Stress state parameters in the northwest flank of Pacific, region Honshu – southern Kurile islands:
a– geodynamic regime type and orientation of dip of maximal compression axis σ_3;
b– effective pressure and orientation of minimal stress axis σ_1 dip.
In the insets are shown: A, C – circular diagrams of azimuths and dip angles of principal stress axes σ_3 and σ_1 accordingly; B – diagram of occurrences of geodynamic regime types in domains; D – diagram of occurrences of effective pressure p^* in domains; E – plot of modulus of maximal shear stresses versus effective pressure.

STRESSES IN REGIONS OF STRONG EARTHQUAKE PREPARATION

The Sumatra-Andaman earthquake, December 26, 2004

This catastrophic earthquake – M_W = 9.3, rupture length 1250 km [Bilham, 2004; Lay *et al.*, 2005] – occurred on the western flank of Sunda seismic region. The fault plane dips gently under Sumatra and Nicobar islands, and its strike azimuth is 329°. We evaluated the stresses in the region of its preparation. For this purpose, solutions from Harvard CMT catalog (http://www.globalcmt.org) (best double-couple) within magnitude range $4.7 \leq M_b \leq 6.5$, located on the western flank of Sunda arc at depths up to 60 km and within the time-interval 1971 - October 2004 were used. The solutions for 220 earthquakes were used in the calculations. The

range of magnitudes and the spatial distribution of earthquakes correspond to the spatial resolution of the stress evaluation equal to 50-100 km in lateral direction [Rebetsky and Marinin, 2006a, b]. Application of the MCA algorithm was carried out for grid nodes 0.5°x0.5° located at 30 km depth. Homogeneous sets of earthquake mechanisms were compiled for 114 quasi-homogeneous earth crust domains.

Results of calculations show that the geodynamic regime varies from north to south in the western flank of the Sunda arc. The crust in the central part of Sumatra island was submitted to horizontal compression (reverse fault tectonics). The orientation of the principal axes was typical for subduction zones [Rebetsky, 2007a, 2009a]. Maximal compression axis σ_3 steeply dips beneath oceanic plate (fig. 2a) and minimal stress axis σ_1 (deviatoric tension) more gently dips beneath sub-continental plate (fig. 2b). The intermediate axis of principal stress σ_2 in such regions is sub-horizontal and strikes parallel to the trench. Further to the north, from Sumatra island up to Nicobar islands, where the seismoactive zone turns from the trench axis toward the sub-continental plate, the intermediate principal stress axis σ_2 becomes sub-vertical. This corresponds to a horizontal shearing stress regime (strike-slip tectonics). In the back-arc basin to the east from Andaman islands in the pull-apart structures, the axis of maximal compression is sub-vertical, which indicates a regime dominated by horizontal extension (normal fault tectonics).

The spatial distribution of orientation of principal stress axes demonstrates that crustal stresses in the western flank of the Sunda arc prevailing before the main shock were generated both by the underthrusting of the oceanic plate below the sub-continental one and by the southward motion of the Burma plate along the Andaman-Nicobar and Central Sumatra strike-slip faults.

The directions in which shear stresses τ_z act on horizontal planes having downward normal are shown in fig. 2b. These underthrusting shear stresses reflect the impact of the mantle at the base of the crust. In the area to the south from Nias island their orientation is typical for subduction zones, from oceanic plate toward the sub-continental one. From the northern edge of Sumatra island up to Nicobar islands the orientation of these stresses is reversed. Chaotic orientations of underthrusting shear stresses in the region of Andaman islands and pull-apart structures and small ratio of τ_z/τ reflect sub-vertical orientations of principal stress axis σ_2 and σ_3.

Application of the MCA second and third stages makes it possible to evaluate the internal cohesion of rock massifs [Rebetsky and Marinin, 2006a,b; Rebetsky, 2009a,b,c]. For the calculations we assumed a mean stress drop $\Delta\tau_n \approx 0.9$ MPa for the initial part of the main shock source ($L_q = 420$ km and $W_q = 240$ km). The seismic moment $M_o = 4\ 10^{22}$ Nm corresponds to this initial part [Bilham, 2005; Lay *et al.*, 2005]. The stress drop was calculated using the relationships linking the seismic moment to the dynamic and geometric parameters of the source ($\Delta\tau_n = \chi M_o / (W_q L_q^2)$ where $\chi = 1.85$) [Kostrov and Das, 1988].

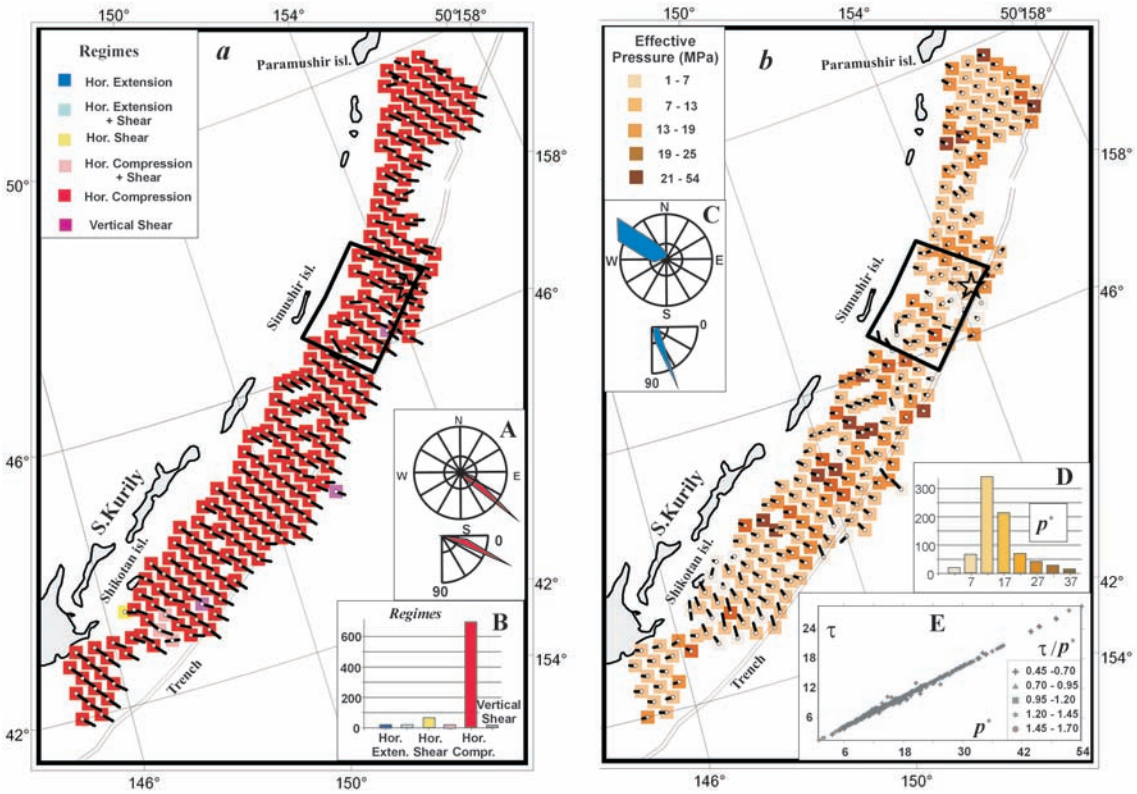

FIG. 4. – Stress state parameters of the northwestern flank of the Pacific, region of Kurile islands:
a– geodynamic regime type and orientation of dip of maximal compression axis σ_3;
b– effective pressure and orientation of minimal stress axis σ_1 dip.
In the insets are shown: A, C – circular diagrams of azimuths and dip angles of principal stress axis σ_3 and σ_1 accordingly; B – of occurrences of geodynamic regime types in domains; D – diagram of occurrences of effective pressure p^* in domains; E – plot of modulus of maximal shear stresses versus effective pressure

Fourteen domains with defined stress-state parameters (ca. 25% of surface) correspond to the initial part of the Sumatra-Andaman main shock having 450 km length (polygon in fig. 2), where 70% of energy of seismic waves was released (M_w = 9.0 corresponds to this segment [Bilham, 2004]). For these nodes the mean reduced stress drop was calculated $\langle \Delta\tau_n / T_f \rangle = 0.26$. Other nodes along oceanic trench were characterized by relatively low seismic activity with a few data on earthquake source mechanisms. Such situation can be interpreted as follows: the stress state there is far from being critical at the scale for which stresses were averaged for calculations. Taking this into account we assume $\langle \Delta\tau_n / T_f \rangle \approx 0$ for these areas. The mean for the source internal cohesion value $T_f \approx 3.5$ MPa is evaluated using stress drop assessment from seismological data and the average value $\langle \Delta\tau_n / T_f \rangle = 0.26$.

Data on τ_f make it possible to evaluate stresses acting along the seismoactive zone before the Sumatra-Andaman earthquake. Effective confining pressure p^* varies within a wide range (fig. 2b). The lowest values (less than 15 MPa) were in the region between Nias and Nicobar islands extending ca. 300-400 km. From the south this zone borders the region of high values of confining pressure (ca. 50 MPa) extending over 200-250 km. The nucleation point of the Sumatra-Andaman earthquake source was located on the boundary between the regions of high and low confining pressure, i.e. in the zone of high gradient.

According to the results of laboratory experiments on rock failure [Byerlee, 1968; Brace, 1978] regions of high effective pressure are characterized also by higher deviatoric stresses. The MCA application experience demonstrates that the ratio between the modulus of the maximal shear stress τ and the effective pressure p^* varies within the range 0.5-2 (fig. 2b, inset G). It has to be noted that the *rupture did not propagate* toward the region of higher deviatoric stresses (to the south and south-east) where the effective pressure is also high, but toward mean and low values (north, north-west) where the confining pressure is low. This segment is characterized also by lower friction forces. Therefore, a minor part of elastic deformation energy will be spent for heating the activated rupture segment while a major part will be left to do the work for further *rupture propagation*.

According to the seismological data [Ammon *et al.*, 2005] rupture propagated with 2.0 km/sec velocity the first 100 km, radiating a little energy in seismic waves. High values and gradient of confining pressure correspond to this region in figure 1b. Rupture velocity increased up to 2.5 km/sec and seismic radiation was maximal for the next 350 km, characterized by lower stresses (both deviatoric and isotropic). Closer to Nicobar islands the seismic radiation drops abruptly and the moment-rate density decreases. This segment is characterized by higher effective pressure located to the east from the trench.

The Tokachi-oki earthquake, September 25, 2003

The JMA earthquake catalogue (http://158.203.31.121/ freesia/ event/search/search.html) for the time-period 01.01.1997 – 25.09.2003 was used to reconstruct the state of stress in the source zone of the Tokachi-oki earthquake M_w = 8.3 which occurred to the southeast from Hokkaido island. The earthquake fault plane dips gently (7°) under Hokkaido island, striking 234°; source dimensions along the oceanic trench are 180 km, 150 km across strike (http://neic.gov/neis/ eq_depot//2003). For the time-period 01.01.1997 - 25.09.2003, 1500 fault-plane solutions within the magnitude range $5.5 \geq M_w \geq 3.5$ are available. Stress reconstruction using the MCA algorithms was carried out for grid nodes 0.1°×0.1° located at 20 km depth (source depth is 27 km); corresponding stress parameters are averaged within 10-20 km cells [Rebetsky, 2009b, c].

Results of the stress-state reconstruction for the earth crust under Japan and Kuril islands are shown in figure 3. The orientation of principal stress axes is typical for subduction zones. Horizontal compression dominates (fig. 3a); combination of horizontal compression and shearing (reverse and strike-slip fault tectonics) and vertical shearing (vertical normal or reverse fault tectonics) are locally observed too. Almost all of them fall into the source zone of the 04.10.1994 Shikotan earthquake M_w = 8.3 (in the region of southern Kuril islands) or in the preparation region of the Tokachi-oki earthquake. Note also that horizontal extension prevails in the segment near the trench in southern Kuril islands. Such a change from horizontal compression at the contact zone of continental and oceanic plates (oceanic trench) to horizontal extension in the oceanic lithosphere is also typical for subduction zones.

For evaluation of the stresses we use data on seismic moment $M_o = 1.5\ 10^{21}$ J, on radiated energy in seismic waves $E_s = 1.7\ 10^{16}$ J, and shear module $\mu = 4\ 10^{10}$ Pa. Then according to ($\Delta\tau_n = 2\mu\, E_s/M_o$) we got a mean value for stress drop of $\Delta\tau_n$ = 0.9 MPa. Using the MCA algorithm we got the mean reduced stress drop (0.5) and based on it we assessed an averaged (within the 100-200 km cell) internal cohesion $T_f \approx 1.8$ MPa. The stress parameters for Tokachi-oki earthquake source zone were evaluated for 27 domains (40% of the area).

We estimate that the confining effective pressure and the maximal shear stresses in the source zone are characterized by mean values of 3-20 MPa and 1-10 MPa, respectively. The preparation zone of the Tokachi-oki earthquake is characterized by a rather homogeneous stress state. The nucleation point coincides with the segment where effective pressure is minimal – 3-4 MPa – close to the rectangle center in figure 3b. The *rupture propagated* upward and downward (under Hokkaido island) along the trench axis. Probably the zones of higher effective confining pressure in northeast and southwest (15-20 MPa and 5-25 MPa) hampered its further propagation.

The Simushir island earthquake, November 15, 2006

The basic data for compilation of the catalogue of source mechanisms for Kurile region [Rebetsky, 2009a] come from the Harvard CMT catalog (http://www.globalcmt.org). It included 1200 earthquakes with $M_w \geq$ 4.7, which occurred in the period from 1976 to June 2006 at depths up to 60 km. The catastrophic Simushir island earthquake M_w = 8.3 (http://neic.gov/neis/eq_depot//2006) occurred in the middle part of the Kurile islands at 30 km depth. The polygon in figure 4 shows the source zone of the Simushir island earthquake according to the NEIC data [Tikhonov *et al.*, 2007] on its aftershocks.

The earthquake fault plane strikes 214° and dips 15° under the Kurile islands. In the region there were 26 earthquakes in this time-period with magnitude more than 7 including

the Shikotan earthquake. Magnitude interval and spatial distribution of earthquakes make it possible to reconstruct the stress state parameters with 30-50 km resolution. Reconstruction was carried for 0.2°×0.2° spatial grid nodes located at 20 km depth. The study region includes also part of southern Kurile islands, for which the JMA seismological data was available.

The orientation of the principal stress axes along central and southern part of Kurile islands is typical for subduction zones; it corresponds to a regime of horizontal compression (fig. 4a). There are some local deviations fromt his regime in the source zone of the Shikotan earthquake. There are 145 domains with defined stress parameters for the earthquake source zone extending 240 km along the trench (polygon in fig. 4). These domains cover 85-90% of the source. The following seismological data on the Simushir earthquake was used for evaluation of the mean internal cohesion (http://neic.gov/neis/eq_depot//2006): energy radiated through seismic waves E_s (7.4 10^{16} J) and seismic moment M_o (3.4 10^{21} J). Based on this data the stress drop is $\Delta\tau_n$ = 1.7 MPa, and, according to the third stage of the MCA algorithm, effective cohesion is T_f = 1.2 MPa.

Results of the stress state reconstruction reveal (fig. 4b) that the region is characterized by a mosaic distribution of effective confining pressure (along Iturup and Urup islands). At the same time there are rather large segments (150-200 km) where this parameter is stable and is within the range of 5-15 MPa, which corresponds to the mean level. These are segments near Shikotan, Simushir, Paramushir islands and junction of Aleutian and Kamchatka subduction zones. The nucleation point of the Simushir earthquake rupture is located near the northeastern edge of the region characterized by higher effective pressure. Southern and northern edges of source zone are located in regions of essentially increased effective pressure. The *rupture propagates* from the region of high gradients of stresses toward domains characterized by low effective compression.

It has to be noted that in the source region of the Shikotan 1994 earthquake according to the JMA data, there is also an area of low effective stresses (fig. 3b). In calculations shown in figure 4b based on source mechanism solutions, this anomaly is observed both before and after the Shikotan earthquake occurrence.

Chile (Maule region) earthquake, February 27, 2010

The stress-state reconstruction along the Pacific plate subduction zone near South America was done for the analysis of stresses acting before the Maule earthquake (M_W = 8.8) occurred at 35 km depth. The rupture plane dips gently (18°) under South-American plate; strike azimuth is 18° (http://neic.gov/neis/eq_depot//2010). Regional source

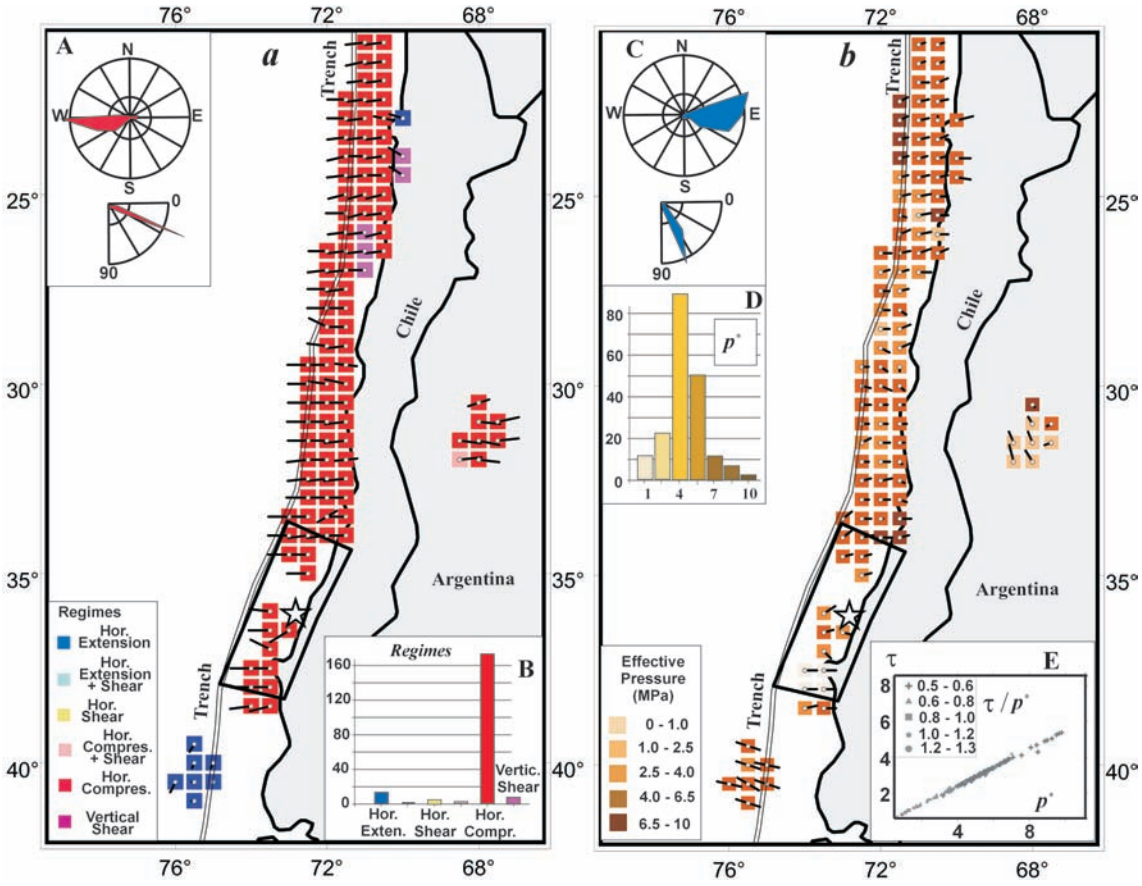

FIG. 5. – Stress state parameters of the Pacific plate subduction zone near South America:
a– geodynamic regime type and orientation of dip of maximal compression axis σ_3;
b– effective pressure and orientation of minimal stress axis σ_1 dip.
In the insets are shown: A, C – circular diagrams of azimuths and dipping angles of principal stress axis σ_3 and σ_1 accordingly; B – diagram of occurrences of geodynamic regime types in domains; D – diagram of occurrences of effective pressure p^* in domains; E – plot of modulus of maximal shear stresses versus effective pressure.

mechanism catalogue was compiled based on the Harvard CMT catalog (http://www.globalcmt.org). The catalogue of mechanisms contains 656 solutions for $M_w \geq 4.8$ earthquakes occurred up to the 60 km depth in the time-interval 01.01.1976 - 01.06.2009.

Results of reconstruction shown in figure 5a indicates that there are only two crust domains where the stress state type differs from that of the subduction one. These are coastal areas of southeastern Peru and southern Chile, where the stress regime is close to horizontal extension. The sharp change in the direction of principal stress axis and of underthrusting shear stresses in the northwestern region of the reconstruction area is noticeable. The same kind of variation in the underthrusting shear stresses is observed in the continental part at latitude 28°S. It may reflect the changes in the direction of crust motion relative to the mantle. Our data on stresses does not allow us to define unequivocally how deformations evolve in the transition zone from mantle to the crust, i.e., by coupling or decoupling.

Seismological data on scalar seismic moment M_o and energy radiated through seismic waves E_r for preceding earthquakes in August 15, 2008 (M_w = 0.8), November 4, 2007 (M_w = 7.8), and the Maule earthquake (http://neic.gov/neis/eq_depot) was used for calculation of the stress absolute values and evaluation of the effective cohesion strength. Using this data, the mean shear stress released ($\Delta\tau_n$) in the sources of these earthquakes was calculated. It varies from 0.2 to 0.3 MPa. From the other hand the mean reduced stress-drop $\left\langle \Delta\tau_n / T_f \right\rangle$ is equal to 1.1 for the crust domains where stresses were evaluated. Based on this data, the mean internal cohesion is evaluated to be $\tau_f \approx 3$ MPa and also absolute values of stresses were assessed.

The distribution of the effective pressure reflecting the stress-state averaged for the whole time-period (from 01.01.1976 to 27.02. 2010) is shown in figure 5b. The Maule earthquake 500 km long source is located in the region of low effective pressure level (low Coulomb friction) and rupture nucleation point is close to the local gradient of effective pressure. The *rupture propagates* from local high stress area to the surrounding volume of low effective compression. The high effective pressure region to the north from the source can be interpreted as a crustal volume with a high Coulomb friction, which hampered propagation of the rupture in this direction. To the south from the source there is also a region of higher effective pressure, but the rupture has stopped at 200 km distance before it, in the region where there is no information on the stress state because of the lack of strong earthquakes there. Indirectly, it is an argument to assess a low level of deviatoric elastic stresses.

DISCUSSION

The results of stress reconstruction in the source zones of preparation of strong earthquakes can be interpreted in the following way. The strong earthquake source is forming in the crust region with low effective confining pressure. The size of the region determines the magnitude of the future strong earthquake. Usually, such zones are limited from both sides or from one side by crust areas characterized by high effective pressure. The rupture nucleation point is located either at the edge of low effective pressure zone where the gradient is maximal (the Sumatra – Andaman and the Simushir earthquakes) or in its central part where effective pressure can locally increase (the Maule earthquake) or within the zone of minimal effective pressure (the Tokachi-oki earthquake). The rupture propagates toward the domains with the lowest level of effective compression [Rebetsky, 2007b].

We consider that such situation is not random. The presence of gradients in stress distribution and extended zone of low effective pressure defines conditions for large-scale brittle failure. According to the Mohr's diagram, when the rupture develops into the zone of low confining pressure (the arrow from point C of figure 1a) the stress drop increases and, so does the release of elastic deformation energy. And the opposite, when rupture moves toward higher level of deviatoric stresses and confining pressure, the release of energy of elastic deformation decreases.

In the plasticity theory the Mises criterion is well known [Mises, 1928]. It states that among all possible variants of plastic processes, the one which ensures maximum energy dissipation will actually be realized. One can suggest that a somewhat similar principle is valid also for brittle failure: in the inhomogeneous stress state zone, the process, at the beginning, develops toward the region where energy (accumulated in elastic deformations) release is maximal. Note that we are not talking about the volume where more energy is accumulated in elastic deformations, but where more energy will be released in seismic waves. For Coulomb's media, which is the case for crustal rocks, these are always different places. This principle determines *rupture propagation* toward lower effective pressure and deviatoric stresses, when the rupture nucleation is located within the high stress region (arrow along the envelope in the right side of figure 1a).

When applied to the rocks the principle of extremum has to consider not the complete deviatoric energy of elastic deformations but its part, which is released through brittle failure. Thus, fault segments along which stress intensity is highly variable should be considered as regions of instability, potentially ready for occurrence of dynamically propagating extensive ruptures. The region of low stresses surrounded by regions of high stresses defines minimal rupture length and correspondingly the minimal earthquake magnitude.

The region of high stress gradients is the place where the nucleation of the future strong earthquake source can be expected. When in the zone of high gradients the stress distribution at different scales becomes smoother, the region is closer to the meta-stable state [Gol'din, 2004]. They are more dangerous when the low level of stresses turns to be more homogeneous (disappearing zones of high confining pressure).

Any seismic impulse that occurred there can trigger a strong earthquake, which source at least will correspond to the stress gradient region. Without meeting patches for destruction of which the energy has to be spent, the *rupture propagates* with increasing velocity and energy accumulated in seismic waves. Further, penetrating into the low effective pressure regions where also the friction is low, rupture breaks local zones of high friction (pressure) using accumulated kinetic energy. The rupture stops either when it meets a large area of high effective pressure or when it gradually spent the energy passing through the region of low deviatoric stresses.

Acknowledgments. – Research is partly supported by the Russian Foundation of Basic Research (RFBR) grants 06-05-644109, 07-05-00106, 09-05-01022, 11-05-00361 and n°6 DSE RAS program.

References

AMMON C.J., JI C., THIO H.-K. *et al.* (2005). – Rupture process of the 2004 Sumatra-Andaman Earthquake. – *Science*, **308**, 1133-1139.

ANGELIER J. (1975). – Sur l'analyse de mesures recueillies dans des sites faillés : l'utilité d'une confrontation entre les méthodes dynamiques et cinématiques. – *C. R. Acad. Sci.*, Paris, D, **281**, 1805-1808.

ANGELIER J. **(**1989). – From orientation to magnitude in paleostress determinations using fault slip data. – *J. Struct. Geol.*,**11**, ½, 37-49.

ANGELIER J. & MECHLER P. (1977). – Sur une méthode graphique de recherche des contraintes principales également utilisable en tectonique et en séismologie: la méthode des dièdres droits. – *Bull. Soc. géol. Fr.*, **XIX**, 6, 1309-1318.

ARTHAUD F. (1969). – Méthode de détermination graphique des directions de raccourcissement, d'allongement et intermédiaire d'une population de failles. – *Bull. Soc. géol. Fr.*, 7, **XI**, 729-737.

BILHAM R. **(**2004). – A flying start, then a slow slip. – *Science*, **308**, 1126-1127.

BRACE W.F. **(**1978). – Volume changes during fracture and frictional sliding. – *A Rev. Pure Appl. Geophys.*, **116**, 603-614.

BYERLEE J.D. **(**1968). – Brittle-ductile transition in rocks. – *J. Geophys. Res.*, **73**, 14, 4741-4750.

CAREY E. (1976). – Analyse numérique d'un modèle mécanique élémentaire appliqué à l'étude d'une population de failles: calcul d'un tenseur des contraintes à partir des stries de glissement. – Thèse, Univ. Paris Sud.

CAREY-GAILHARDIS E. & MERCIER J.L. **(**1987). – A numerical method for determining the state of stress using focal mechanisms of earthquake populations: application to Tibetan teleseismic and microseismicity of southern Peru. – *Earth Planet. Sci. Let.*, **82**, 165-179.

CASTRO R.R, ANDERSON J.G. & SINGH S.K. (1990). – Site response, attenuation and source spectra of S waves along the Guerrero, Mexico, subduction zone. – *Bull. Seismol. Soc. Am.*, **80**, 1481-1503.

CHERNYKH K.F. (1988). – Introduction to anisotropic elasticity. – Nauka Press, Moscow, 190 p. (in Russian).

ETCHECOPAR A., VASSEUR G. & DAIGNIÈRES M. (1981). – An inverse problem in microtectonics for the determination of stress tensors from fault striation analysis. – *J. Sruct. Geol.*, 3, 51-65.

GEPHART J.W. & FORSYTH D.W. (1984). – An improved method for determining the regional stress tensor using earthquake focal mechanism data: application to the San Fernando earthquake sequence. – *J. Geophys. Res.*. **89**, B11, 9305-9320.

GINTOV O.B. (2005). – Field tectonophysics and its application for research of crustal strain of Ukraina. – Kiev, Feniks Press, 572 p. (in Russian).

GINTOV O.B. & ISAI V.M. (1984). – Some laws fault forming and a technique morphocinematic the analysis of strike-slip faults. – *Geophys. J.*, **6**, 3, 3-10. (in Russian).

GOL'DIN S.V. **(**2004). – Dilatance, re-compaction and earthquake. – *Phys. Earth.*, **10**, 37-54 (in Russian).

GOUSTCHENKO O.I. (1975). – The kinematic principle of reconstruction of directions of the principal stresses (under the geological and seismological data). – *Rep. Acad. Sci. USSR*, Ser. Geophys., **225**, 3, 557-560 (in Russian).

HAIN V.E. & LOMIZE M.G. (1995). – Geotectonicswith elements of geodynamics. – Moscow. MSU Press, 480 p. (in Russian).

HARDEBECK J.L. & HAUKSSON E. (2001). – Crustal stress field in southern California and its implications for fault mechanics. – *J. Geophys. Res.*, **106**, B10, 21859-21882.

JAGER J.C. (1962). – Elasticity fracture and flow. – London, Methuen & Co, LTD, 208 p.

JAMAJI A. (2000). – The multiple inverse method: a new technique to separate stress from heterogeneous fault-slip data. – *J. Struct. Geol.*, **22**, 411-452.

KASAHARA K. **(**1981). – Earthquake mechanics. – Cambridge Univ. Press, 250 p.

KOSSOBOKOV V.G. & KEILIS-BOROK V.I. (1990). – Localization of intermediate-term earthquake prediction. – *J. Geophys. Res. B.*, **95**, 12, 763-772.

KOSTROV B.V. & DAS SH. (1988). – Principles of earthquake source mechanics. – Cambridge Univ. Press, 174 p.

LAY T., KANOMORY H., AMMON C.J. *et al.* (2005). – The great Sumatra-Andaman earthquake of 26 December 2004. – *Science*, **308**, 1127-1133.

LISLE R. (1979). – The representation and calculation of the deviatoric component of geological stress tensor. – *J. Struct. Geol.*, **1**, 317-321.

LOVE A.E.H. (1927). – A treatise on the mathematical theory of elasticity. – Cambridge Univ. Press.

MICHAEL A.J. (1984). – Determination of stress from slip data: faults and folds. – *J. Geophys. Res.*, **89**, B11, 11517-11526.

MISES R. VON Z. (1928). – *Angew. Math. Mech.*, **8**, 161-185.

MJACHKIN V.I., BRACE W.F., SOBOLEV G.A. & DIETERICH J.H. (1975). – Two models for earthquake forerunners. – *Pure. Appl. Geophys.*, **113**, 169-181.

MOGI K. (1966). – Pressure dependence of rock strength and transition from brittle fracture to ductile flow. – *Bull. Earth Res. Inst.*, Univ. Tokyo, **44**, 215-232.

OSOKINA D.N. (1988). – Hierarchical properties of a stress field and its relation to fault displacements. – *J. Geodyn.*, **10**, 331-344.

PANIN V.E. (1998). – Basis of mesomechanics. – *Phys. Mesomechanics*, **1**, 1, 5-22. (in Russian).

PEGORARO O. (1972). – Application de la microtectonique à une étude néotectonique sur le golfe Maliaque (Grèce centrale). – Thesis University of Montpellier.

REBETSKY YU. L. (1996). – I. Stress-monitoring: Issues of reconstruction methods of tectonic stresses and seismotectonic deformations. – *J. Earthquake Predict. Res.*, Beijing, **5**, 4, 557-573.

REBETSKY YU. L. (1997). – Reconstruction of tectonic stresses and seismotectonic strain: Methodical fundamentals, current stress field of southeastern Asia and Oceania. – *Doklady Earth. Sci.*, **354**, 4, 560-563.

REBETSKY YU. L. **(**1999). – Methods for reconstructing tectonic stresses and seismotectonic deformations based on the modern theory of plasticity. – *Doklady Earth Sci.*, **365A**, 3, 370-373.

REBETSKY YU. L. **(**2001). – Principles of stress monitoring and method of cataclastic analysis discontinue dislocation. – *BMOIP*, ser. geol., **76**, 4, 28-35 (in Russian).

REBETSKY YU. L. **(**2003). – Development of the method of cataclastic analysis of shear fractures for tectonic stress estimation. – *Doklady Earth Sci.*, **388**, 1, 72-76.

REBETSKY YU. L. (2005a). – Evaluation of the relative values of the stress – the second stage of reconstruction according to the discontinuous displacements. – *Geophys. J.*, **27**, 1, 39-54 (in Russian).

REBETSKY YU. L. **(**2005b). – Tectonic stress, metamorphism, and earthquake source model. – *Doklady Earth Sci.*, **400**, 1,127-131.

REBETSKY YU. L. (2007a). – Tectonic stress and the strength of rock. – Moscow, Sci. Press, 406 p. (in Russian).

REBETSKY YU. L. **(**2007b). – Stressed state corresponding to formation of large-scale brittle failure of rock. – *Doklady Earth Sci.*, **417**, 8, 1216-1220.

REBETSKY YU. L. (2009a). – Stress state of the Earth's crust of the Kurils islands and Kamchatka before the Simushir earthquake. – *Russ. J. Pacific Geol.*, **3**, 5, 477-490.

REBETSKY YU. L. (2009b). – Estimation of stress values in the method of cataclastic analysis of shear fracture. – *Doklady Earth Sci.*, **428**, 7, 1202-1207.

REBETSKY YU. L. (2009c). – The third and fourth stages of the reconstruction of the stresses in the method of cataclastic analysis of fault slip data. – *Geophys. J.*, **31**, 2, 93-106 (in Russian).

REBETSKY YU. L. & MARININ A.V. **(**2006a). – Stress state of Earth's crust in the western region of Sunda subduction zone before the Sumatra-Andaman earthquake on December 26, 2004. – *Doklady Earth Sci.*, **407**, 2, 812-815.

REBETSKY YU. L. & MARININ A.V. **(**2006b). – Preseismic stress field before Sumatra-Andaman earthquake of 26.12.2004. A model of metastable state of rocks. – *Russian Geol. and Geophys.*, **47**, 11, 1173-1185.

RECHES Z. (1978). – Analysis of faulting in three-dimensional strain field. – *Tectonophys*ics, **47**, 109-129.

RECHES Z. (1987). – Determination of the tectonic stress tensor from slip along faults that obey the Coulomb yield condition. – *Tectonics*, **6**, 6, 849-861.

REID H.F. **(**1910). – The mechanism of the earthquake. The California earthquake of April 18, 1906. – Rept. of the state investigation commission, Washington, **2**, pt. 1, 56 p.

RICE J. (1979). – The mechanics of earthquake rupture. *In*: Physics of the earth's interior. – Proceedings of the Intern. School of Phys. "Enrico Fermi", Course 78, Italian Phys. Soc., 555-649.

RIVERA L. & CISTERNAS A. **(**1990). – Stress tensor and fault plane solutions for a population of earthquakes. – *Bull. Seism. Soc. Am.*, **80**, 3, 600-614.

SADOVSKY M.A. & PISARENKO V.F. (1985). – Dependence of manifestation time of aharbinder at most earthquake. – *Doklady Acad. Sci. USSR.*, **285**, 6, 1359-1361 (in Russian).

SCHOLZ C.H., SYKES L.R. & AGGARAWAL Y.P. (1973). – Earthquake prediction: A physical basis. – *Science*, **181**, 803-810.

SIBSON R.H. (1974). – Frictional constraints on thrust, wrench and normal faults. – *Nature*, **249**, 5457, 542-544.

SOBOLEV G.A. (1993). – Basis if earthquake prediction. – Nauka Press, Moscow, 312 p. (in Russian).

STAVROGIN A.N. & PROTOSENIA A.G. (1992). – Mechanics of deformation and destruction of rocks. – Moscow, Nedra Press, 1223 p. (in Russian).

TERZAGHI K. (1943). – Theoretical soil mechanics. – John Wiley and Sons, New York.

TIKHONOV I.V., VASILENKO N.F., PRYTKOV A.S., SPIRIN A.I. & FROLOV D.I. (2007). – Catastrophic Simushir earthquakes 15 November 2006 and 13 January 2007. – Coll. Probl. Seism. Hazard. Far East and East Siberia. IMGG DVO RAS Press, South-Sahalin, 27-28 (in Russian).

YUNGA S.L. **(**1979). – Of the mechanism of deformation of seismo-active volume of Earth's crust. – *Izv., Ph. Solid Earth, Eng. Tr. Fiz. Zem.*, **15**, 10, 639-699.